DE GRUYTER Green Processing and Synthesis 2023; 12: 20230084

Research Article

Ratima Waitongkham, Yutthapong Pianroj, Teerasak Punvichai, Seppo Karrila,
Parinuch Chumkaew, and Saysunee Jumrat*

Characterization of bio-oil production by microwave pyrolysis from cashew nut shells and *Cassia fistula* pods

https://doi.org/10.1515/gps-2023-0084
received May 23, 2023; accepted July 24, 2023

Abstract: In this study, the production of bio-oil by pyrolysis with microwave (MW) heating was tested experimentally. Two magnetrons with a total MW power of 1,600 W were used in the pyrolysis setup. The electric field strength was 185.38 V·m^{-2} at an MW frequency of 2.45 GHz. Cashew nut shells (CNS) or *Cassia fistula* pods (CFP) were pyrolyzed at 400°C, 500°C, or 600°C, with biomass-to-activated carbon ratio set at 70:30, 80:20, or 90:10. The largest yield of bio-oil was found for CNS at 600°C, and for CFP at 500°C, both with 90:10 ratio, achieving, respectively, 20.0% and 15.8% yields. When the bio-oil yields from CNS and CFP at 90:10 ratio and 400–600°C were analyzed with gas chromatograph-mass spectrometer, the components found included acids, esters, ketones, furans, pyrans, guaiacol, syringol and phenols, and phenolic derivatives were the dominant type of compounds. There were 23.56% and 13.23% phenolic derivatives, respectively, in the bio-oils from CNS (at 500°C) and from CFP (at 400°C). An analysis with Folin–Ciocalteu reagent of the phenolic contents in bio-oils gave the respective ranges 146.83–164.83 mg·GAE·g·DW^{-1} and 39.34–45.91 mg·GAE·g DW^{-1} for CNS and CFP (both run with 90:10 ratio).

Keywords: pyrolysis, bio-oil, phenol, GC-MS, Folin–Ciocalteu

1 Introduction

The reserves of fossil fuels decrease with consumption, and their costs are gradually rising. In addition to the negative environmental effects, concerns about the eventual scarcity of fossil fuels exist. Since agricultural biomass is expected to replace crude oil and other fossil fuels in the future, for practical adoption, it should be converted to biofuels that can substitute for oil-derived products [1]. Biomass is a naturally renewable organic energy source that can be physically stored for use when needed. Bagasse, rice husks, oil palm meal, cashew nut shells (CNS), *Cassia fistula* pods (CFP), wood chips, etc., are a few examples of biomass types used in Thailand. These generally constitute agricultural, industrial, and environmental waste streams [2].

Phenols are required as the major feedstock in the production of phenolic resins, plastics, insecticides, dyes, and fuels [3,4]. Since petroleum compounds are commonly used to produce phenols, the cost and accessibility of phenol feedstocks would be influenced by those of fossil fuels [5]. Many types of natural phenolic compounds differ in chemical structure, ranging from simple structures, such as in phenolic acids, to polymerized structures, such as in lignin [6].

Lignocellulosic biomass is considered a promising renewable energy source that can be transformed into a liquid product, known as bio-oil, through fast pyrolysis, and bio-oil is a promising alternative biofuel. The composition and quality of the bio-oil, which is a complex mixture of

---

*** Corresponding author: Saysunee Jumrat**, Integrated High-Value Oleochemical Research Center, Prince of Songkla University Suratthani Campus, 31 Moo 6, Muang, Surat-Thani, Thailand, 84000, Thailand; Faculty of Science and Industrial Technology, Prince of Songkla University Suratthani Campus, 31 Moo 6, Makhamtia, Muang, Surat-Thani, 84000, Thailand, e-mail: saysunee.j@psu.ac.th

Ratima Waitongkham: Major in Energy Technology, Department of Mechanical Engineering, Faculty of Engineering, Prince of Songkla University Hatyai Campus, 15 Karnjanavanich Road, Hat-Yai, Songkhla, 90112, Thailand

Yutthapong Pianroj: Integrated High-Value Oleochemical Research Center, Prince of Songkla University Suratthani Campus, 31 Moo 6, Muang, Surat-Thani, Thailand, 84000, Thailand; Faculty of Science and Industrial Technology, Prince of Songkla University Suratthani Campus, 31 Moo 6, Makhamtia, Muang, Surat-Thani, 84000, Thailand

Teerasak Punvichai: Integrated High-Value Oleochemical Research Center, Prince of Songkla University Suratthani Campus, 31 Moo 6, Muang, Surat-Thani, Thailand, 84000, Thailand; Faculty of Innovation Agriculture and Fisheries Establishment Project, Prince of Songkla University Suratthani Campus, 31 Moo 6, Makhamtia, Muang, Surat-Thani, 84000, Thailand

Seppo Karrila, **Parinuch Chumkaew:** Faculty of Science and Industrial Technology, Prince of Songkla University Suratthani Campus, 31 Moo 6, Makhamtia, Muang, Surat-Thani, 84000, Thailand

oxygenated molecules, are greatly influenced by the makeup of the biomass feedstock. Cellulose, hemicellulose, and lignin are the three primary structural constituents in lignocellulosic biomass [7], which have also been investigated as an alternative source of phenols and other phenolic compounds [8,9].

In Thailand, cashew nuts are a significant economic crop, considered an important agricultural product [10]. Most often the CNS are discarded as waste, causing hazardous waste problems in the environment. CNS contains phenols as the main constituent, along with a dark brown viscous oil known as cashew nut shell liquid (CNSL), found in the soft honeycomb structure between the inner and outer shells. CNSL accounts for approximately 30–35% of the total shell weight and is by far the most important component of the shell [11]. Commercially, there are a variety of CNSL extraction methods [12], such as roasting nuts and collecting excreted liquids, extraction of hot CNSL without charring the kernels, superheated steam treatment, and solvent extraction methods. CNSL and its derivatives are reportedly used in polymer-based industries such as friction linings, primers, paints, varnishes, binder resins, cashew cements, adhesives, and polyurethane-based polymers [13]. In addition, CNSL is also used as a feedstock for chemicals, bactericidal agents, antiseptics, insecticides, disinfectants, homogenizing agents, and substances that act on the surface [14,15]. Budaraga et al. [16] reported that CNSL was an alternative material with a high potential to replace phenol in the production of varnishes. Thailand has *Cassia fistula* plants distributed throughout the kingdom, and locals refer to them as “Khun” or “Ratchaphruek.” Usually, when CFPs fall from the tree to the ground, some local villagers use them to produce firewood. This plant produces a lot of pods with brown seeds for which there is no use, and a large quantity of dried pods is discarded annually [17]. According to studies, the pods contain more phenolic compounds than the other parts of *C. fistula* trees [18]. The composition of this biomass has the right properties to create multiple beneficial products, such as solids, liquids, gases, and chemicals, by applying thermochemical processing. Liquefaction, hydrolysis, pyrolysis, or gasification can transform varied biomass wastes into more valuable products [19]. Among the thermochemical methods, pyrolysis is the most interesting one because it has been used in converting a variety of waste biomasses into different products [20].

Pyrolysis is a thermal chemical process that disintegrates organic compounds in the absence of oxygen, yielding liquid, solid, and gaseous products that vary depending on the raw materials and processing conditions used. The liquid produced by pyrolysis can serve as an alternative fuel or as a source of chemicals [21]. The heating rate used in pyrolysis can either be for slow pyrolysis ($0.01–10°C·s^{-1}$) or for fast or flash pyrolysis ($10–1,000°C·s^{-1}$) [22]. During the pyrolysis of lignin, thermal decay occurs over a wide temperature range (160–900°C), and bond breakage occurs randomly along the lateral chains of the aromatic ring and at aromatic bonds, resulting in various phenolic products [23,24]. In pyrolysis fluids, phenols and phenolic compounds have been formed by breaking the phenylpropane units in the lignin fraction of lignocellulose biomass [25]. In recent years, microwaves (MWs) at the commonly adopted 2.45 GHz frequency have been used as optimized heat sources in the pyrolysis of biomass. The results have shown that MW-based dielectric heating can reduce both energy consumption and reaction time so that MW pyrolysis can improve the overall production performance [26,27]. Heat transfer in MW pyrolysis occurs directly inside the raw materials by convection and does not induce surface drying of the raw materials [28] when compared with traditional pyrolysis, which uses heat from electric resistances. Therefore, microwaving is more efficient because it provides rapid volumetric heating [29]. Bio-oil from MW pyrolysis of sewage sludge was much cleaner than the bio-oil produced from traditional pyrolysis, as it did not contain harmful compounds such as heavy aromatic polycyclic compounds [30]. This study used MW oven for heating the samples.

Bio-oil has several environmental advantages compared to fossil fuels, as a clean fuel [31]. Bio-oil has a CO_2/GHG balance of zero. As a result, its use can generate carbon credits. Because plant biomass contains insignificant amounts of sulfur, no SO_x emissions are produced [32]. Bio-oil obtained from pyrolysis can be used for various purposes, such as transportation fuel, heat supply for power generation, or as fuel for boilers, furnaces, stationary diesel engines, and turbines [33]. However, the utilization of bio-oil as a biofuel is limited due to storage instability caused by oxidation, condensation, and polymerization. These impede its use as fuel, so improvements are needed [34].

Therefore, this study recognizes the importance of CNS and CFP, both of which are lignocellulosic biomass and potential renewable energy sources, from which bio-oil can be produced through fast pyrolysis to obtain phenols that are important and valuable raw materials.

2 Materials and methods

2.1 Preparation and characterization of biomass

The biomass used in this study was CNS obtained from the Sriburapha Orchid Plant in Phuket province, and CFP obtained from the Prince of Songkla University, Surat Thani campus. Only pods that had fallen to the ground were sampled, and both CNS and CFP were crushed and passed through a 10 mesh (2.00 mm) sieve, then dried in a hot-air oven at 105°C to reduce the moisture content to ≤10 wt%. The biomass was then sent to the Office of Scientific Instruments and Testing (Prince of Songkla University, Hat-Yai campus) for proximate (in-house method based on ASTM D7582) and ultimate (CHNS/O analyzer) analyses. Moreover, activated carbon (AC) (based on coconut shell) was crushed and passed through a 20 mesh (0.85 mm) sieve, then dried in a hot-air oven at 105°C to reduce its moisture content to ≤8 wt%. It was mixed with each type of biomass (CNS and CFP) in order for the AC to serve as a MW absorbent [35].

2.2 Simulation setup

In this step, an MW pyrolysis system was designed for the production of bio-oil. The COMSOL MultiPhysics™ software was used to simulate the interior of an MW reactor system by numerical calculations approximately solving partial differential equations along with integral equations. The finite-element method used is a good alternative for solving partial differential equations in complex domains and was used here to assess the motions of stationary wave formation by MWs within the system.

2.3 Setup of MW pyrolysis reactor system

The MW pyrolysis system was connected to an MW power supply that provides a pulsed electrical signal generated by a high-voltage transformer to double the voltage, a high-voltage capacitor, and a high-voltage diode that cuts off the signal. This MW pyrolysis system transmits MW energy from two magnetrons on opposite sides. It also used a K-type thermocouple to measure the temperature of the mixture (biomass with AC). This thermocouple was connected to temperature display and data logging by the Shimax Soft program. The MW pyrolysis system is schematically shown in Figure 1.

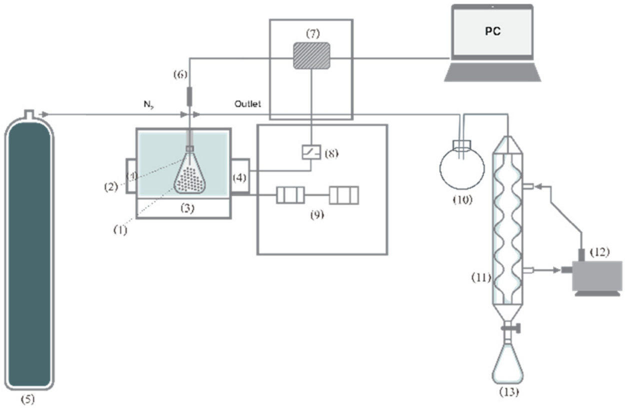

Figure 1: Schematic of experimental MW pyrolysis system: (1) mixture sample, (2) quartz reactor, (3) MW oven, (4) magnetrons, (5) nitrogen tube, (6) thermocouple, (7) microcontroller, (8) solid state relay (SSR), (9) power supply, (10) round bottom flask for storage, (11) condenser, (12) pump, and (13) Erlenmeyer flask for storage.

2.4 MW pyrolysis process

The design of experiments for bio-oil production by MW pyrolysis used factor levels 400°C, 500°C, and 600°C for temperature and biomass (CNS and CFP)-to-AC mass ratio at the levels 70:30, 80:20, and 90:10. The total weight of sample was limited to 500 g in each batch run with the MW pyrolysis reactor. Before starting the MW pyrolysis, flushing with one LPM of pure N_2 gas was done for 5 min to ensure that the ambient air with oxygen had been removed.

2.5 Pyrolysis yield characterization

The bio-oil and the solid char residue were weighed with a digital scale, and the samples were stored in zip-lock bags. The bio-oil was analyzed for total phenolic content (TPC) using Folin–Ciocalteu (FC) reagent, and the chemical composition was otherwise determined with a gas chromatograph-mass spectrometer (GC-MS).

2.6 FC analysis

Gallic acid was used as the reference standard in the concentration range 0–200 $\mu g \cdot mL^{-1}$. Then, the bio-oil samples were diluted to a concentration of 300 $\mu g \cdot mL^{-1}$, and a pipetted solution sample of 20 µL was mixed with 100 µL of FC reagent, then 80 µL of 7.5% Na_2CO_3 was added to the microtiter plate (96 wells). The plate was shaken to ensure good mixing, set aside for 30 min, and the absorbance at 765 nm [36] was measured with a microplate reader, as illustrated in Figure 2. The TPC is reported in milligrams of gallic acid equivalent per gram of dry plant ($mg \cdot GAE \cdot g \cdot DW^{-1}$).

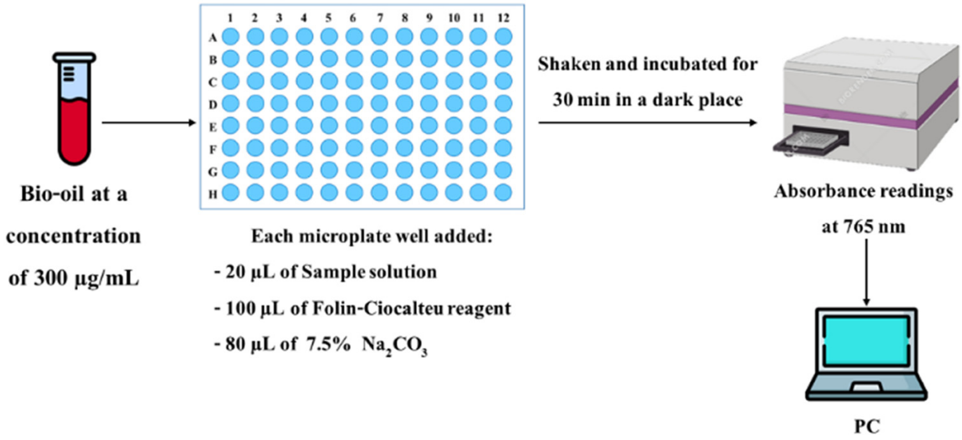

Figure 2: FC analysis of bio-oil with a microplate reader.

3 Results and discussion

3.1 Characteristics of biomass

The results of proximate analysis of CNS and CFP, summarized in Table 1, show higher moisture and more volatiles in CNS than in CFP, while ash and fixed carbon were higher in CFP. Biomass with a high ash content provides better cooling during pyrolysis or combustion than one with a low ash content [37]. Ash consists of minerals and inorganic substances in the biomass and affects the combustion rate of biomass [38]. In addition, biomass with a high ash content produces more residual charcoal from pyrolysis [39]. Table 2 summarizes the ultimate analyses of CNS and CFP, and it can be seen that the heating value and carbon content of CNS were relatively high compared to CFP, which is probably related to the internal CNSL in CNS [40]. The carbon and hydrogen contents are associated with the amount of hydrocarbons released during pyrolysis. Furthermore, it is also widely known that a biomass high in oxygen has a low gross heating value (GHV) [41].

Table 1: Proximate analyses of CNS and CFP

Biomass	Proximate analysis (wt%)			
	Moisture	Volatiles	Ash	Fixed C
CNS	9.650	82.405	1.619	15.972
CFP	4.181	72.003	3.153	20.660

Table 2: Ultimate analyses of CNS and CFP

Biomass	Ultimate analysis (wt%)					GHV ($kcal\cdot kg^{-1}$)	NHV ($kcal\cdot kg^{-1}$)
	C	H	N	S	O		
CNS	57.837	6.809	0.551	0.012	33.924	5,627.917	5,006.659
CFP	45.574	6.115	0.709	<0.01	44.287	3,936.269	3,622.511

3.2 Simulation of the MW pyrolysis system

MW ovens operating at 2.45 GHz frequency can usually be adapted for use in pyrolysis experiments, and some MW modifications were used in this study. The MW pyrolysis system has oven dimensions of 0.22 m × 0.22 m × 0.31 m ($x \times y \times z$). It has two magnetrons with a total output power of 1,600 W (800 W each). The simulation used COMSOL Multiphysics™ software package, based on physical and mathematical models formulated to predict the dynamics of the pyrolysis process run with MW heating. The control equation for the electric field (E) is shown in Eq. 1, in which initial and boundary conditions were enforced in a three-dimensional (3D) numerical model, applying the radio frequency module ≫ electromagnetic waves, frequency domain (emw). The 3D model grid for the MW pyrolysis system of this study is shown in Figure 3a.

$$\nabla \times \mu_r^{-1}(\nabla \times \vec{E}) - k_0^2\left(\epsilon_r - \frac{j\sigma}{\omega\epsilon_0}\right)\vec{E} = 0, \tag{1}$$

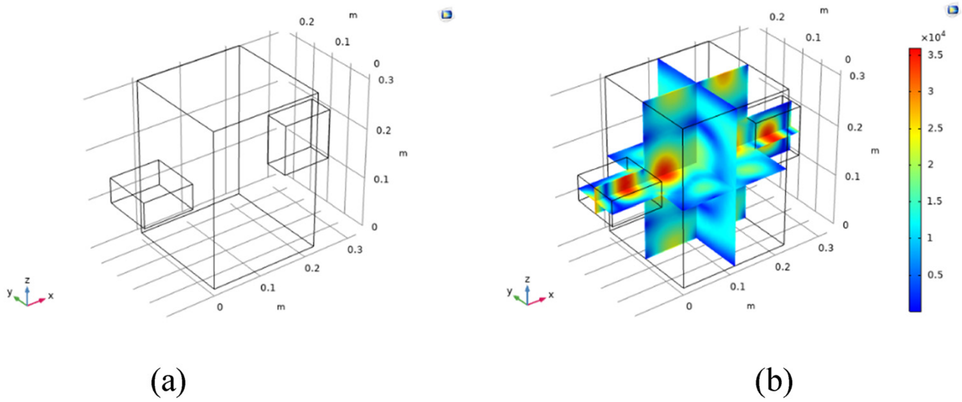

(a) (b)

Figure 3: The 3D simulation model of an MW pyrolysis system (a), and the distribution of MW electric field in the reactor (b).

where μ_r is the relative permeability ($H \cdot m^{-1}$), j is the imaginary unit, σ is the electrical conductivity ($S \cdot m^{-1}$), ω is the angular frequency ($rad \cdot s^{-1}$), k is the thermal conductivity ($W \cdot m^{-1} \cdot K^{-1}$), ϵ_r is the relative permittivity, and ϵ_0 is the permittivity of free space ($F \cdot m^{-1}$). The distribution of the electric field inside the reactor is shown in Figure 3b, and it was found that inside the reactor, there was a total electric field norm (emw.normE) of about 185.38 $V \cdot m^2$.

3.3 MW pyrolysis system

The MW pyrolysis system of this study is shown in Figure 4. It had two magnetrons to transmit MWs from opposing positions, and a K-type thermocouple was used to measure the sample temperature during an experimental batch run.

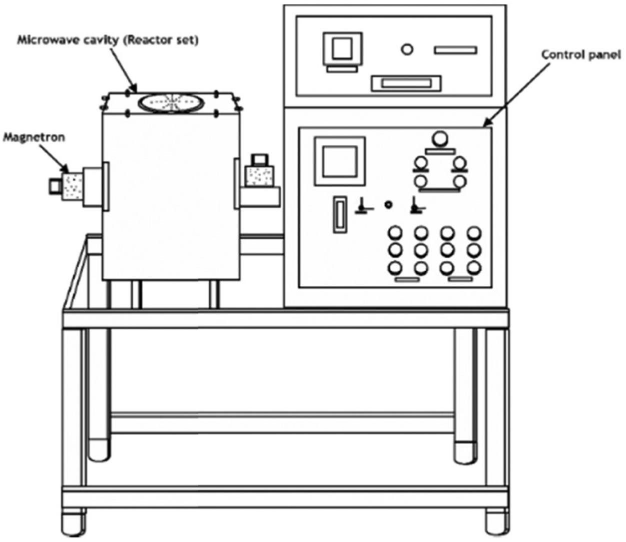

Figure 4: The MW pyrolysis system consists of magnetrons, MW cavity (reactor set), and a control panel.

The digital temperature controller amplified the signal from the thermocouple and regulated the temperature to a setpoint of 400°C, 500°C, or 600°C by manipulating a solid-state relay (SSR). The SSR acts as a circuit breaker turning MW power on and off, and the temperature control implemented did this switching at given maximum and minimum temperatures. The temperature data were recorded by a computer connected *via* RS485 in real-time during each run, using the Shimax software program.

3.4 Pyrolysis yields

The experimental design was done with the Minitab program, and three products were obtained from the MW pyrolysis: solids, liquids, and gases. CNS and CFP were the alternative biomass feedstocks subjected to MW pyrolysis, in which the factors varied were the temperature (400°C, 500°C, and 600°C) and the ratio of biomass (CNS or CFP) to AC MW absorber (70:30, 80:20, and 90:10) as shown in Figure 5. Regarding the yields by product type from MW pyrolysis of CNS and CFP, there were mostly solids, followed by liquids, and finally, gases. The liquid yield from MW pyrolysis of CNS increased with temperature from 400°C to 600°C, namely from 6.0% to 18.7%, while the yield of solids decreased from 72.8% to 46.5%. Although solid products were more abundant than liquid products, this study focused on the yield of phenols found in the liquid products, seen later in the GC-MS results. The liquid (bio-oil) yield from MW pyrolysis of CFP increased with temperature from 400°C to 600°C as well, from 8.1% to 15.3%, while the yield of solids decreased from 79.7% to 56.7%.

When studying the influence of MW pyrolysis with manipulated factors on bio-oil yield (%) from CNS and CFP, it was found that the bio-oil yield of CNS decreased at 500°C, and the yield gradually increased as the temperature

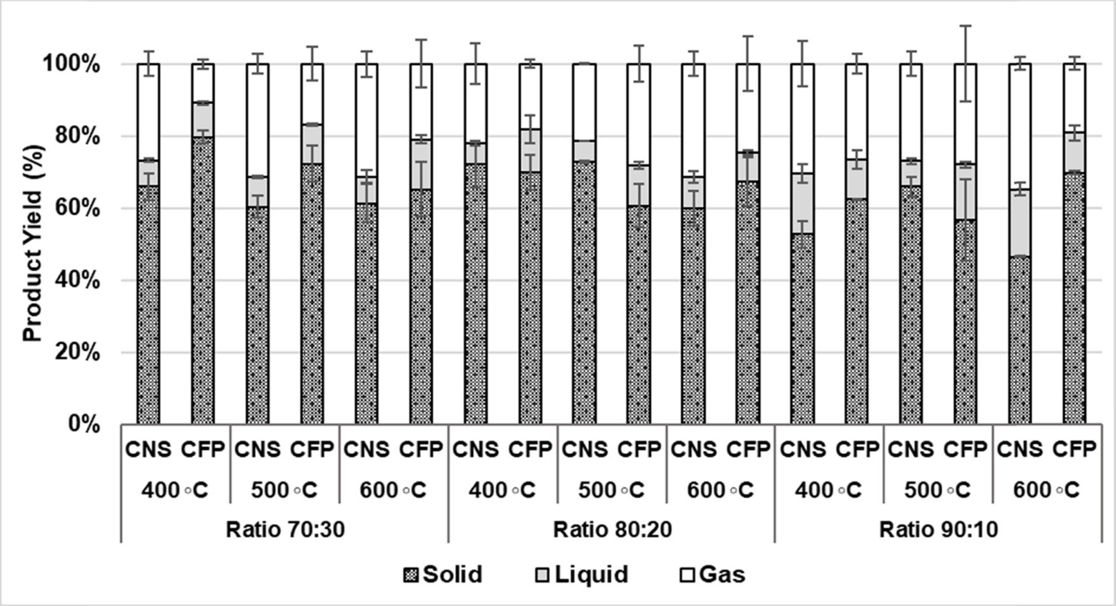

Figure 5: The average product yields (%) obtained from MW pyrolysis of CNS and CFP.

rises, unlike the yield of bio-oils from CFP that increased when the temperature was changed from 400°C to 500°C, but the trend was the opposite when the temperature changed from 500°C to 600°C, giving maximum bio-oil yield at 500°C. The high temperature made the thermal decomposition of biomass complete and easily removed volatile substances, but it also decreased the yield of bio-char. Part of the volatile matter from the biomass can be condensed into bio-oil, while the lighter bio-oil components remain in the gas phase [42]. Guedes et al. [43] reported that the optimum temperature maximizing the liquid product (bio-oil) from pyrolysis depends on the type of biomass feedstock. The yield of solids was similar in trend to other biomass types, such as rice straw and cotton stalk, as biochar amount decreased with pyrolysis temperature. The function of temperature in the pyrolysis process is to decompose the biomass bonds, and the efficiency of biomass decomposition increases with temperature. Numerous studies have discussed the role of temperature in bio-oil yield and stated that temperatures in the range 450–550°C result in higher liquid yields. However, these values change based on the biomass used and other variables in the process [44]. An increase in temperature causes a positive effect on the yield of liquid, but at the same time, if the temperature is very high, there is secondary cracking of volatiles, resulting in a higher gas yield [45]. Regarding the ratio of biomass to AC, increasing the ratio also resulted in increased bio-oil yields from CNS and CFP. AC was an efficient carbon-based catalyst for the production of hydrocarbons during pyrolysis. It enables converting biomass into bio-oil rich in hydrocarbons through a rapid pyrolysis process [46], while not using an MW absorber would only give comparatively slow heating.

Table 3: ANOVAs for the response surface regression models of bio-oil yield (%) from CNS and CFP

Analysis of variance					
Source	**Sum of squares**	**DF**	**Mean square**	***F*-value**	***P*-value**
% yield of CNS					
Model	357.96	7	51.14	19.29	<0.0001
Residual	26.52	10	2.65		
Lack of fit	10.28	1	10.28	5.69	0.0408
Pure error	16.24	9	1.80		
Total	384.47	17			
% yield of CFP					
Model	73.27	7	10.47	3.54	0.0350
Residual	29.57	10	2.96		
Lack of fit	0.3472	1	0.3472	0.1069	0.7511
Pure error	29.22	9	3.25		
Total	102.84	17			

Fit statistics				
Std.Dev.	**Mean**	**C.V. %**	***R*-sq**	***R*-sq (adj)**
% yield of CNS				
1.63	9.88	17.00	0.9310	0.8828
% yield of CFP				
1.72	11.39	15.10	0.7125	0.5112

3.5 Optimization of conditions to maximize bio-oil yield

The maximum yields (in %) of bio-oil from CNS and CFP were assessed. Based on an analysis of variance, the confidence intervals were calculated at 95% ($\alpha = 0.05$) for the fit statistics, with coefficients given for coded factors used by the Design Expert 13 program, as shown in Table 3. For temperatures from 400°C to 600°C, bio-oil from CNS and CFP increased from 6.0% to 18.7% and from 8.1% to 15.3%. The cubic model fits the yield (%) of bio-oil for CNS and CFP, which is shown in Eqs. 2 and 3.

3.5.1 Final equations in terms of coded factor levels

$$\begin{aligned}\%\ \text{Yield of bio-oil from CNS} \\ &= 4.29 + 1.35 \times A - 0.55 \times B + 0.40 \times AB + 3.82 \\ &\quad \times A^2 + 4.12 \times B^2 + 5.80 \times A^2B - 0.90 \times AB^2\end{aligned} \tag{2}$$

$$\begin{aligned}\%\ \text{Yield of bio-oil from CFP} \\ &= 11.38 - 1.90 \times A + 2.25 \times B - 1.08 \times AB - 1.52 \\ &\quad \times A^2 + 1.53 \times B^2 - 2.52 \times A^2B + 3.02 \times AB^2\end{aligned} \tag{3}$$

where A is the temperature and B is the ratio of AC to biomass (CNS or CFP). P-values less than 0.05 indicate terms that are significant in the regression models. The

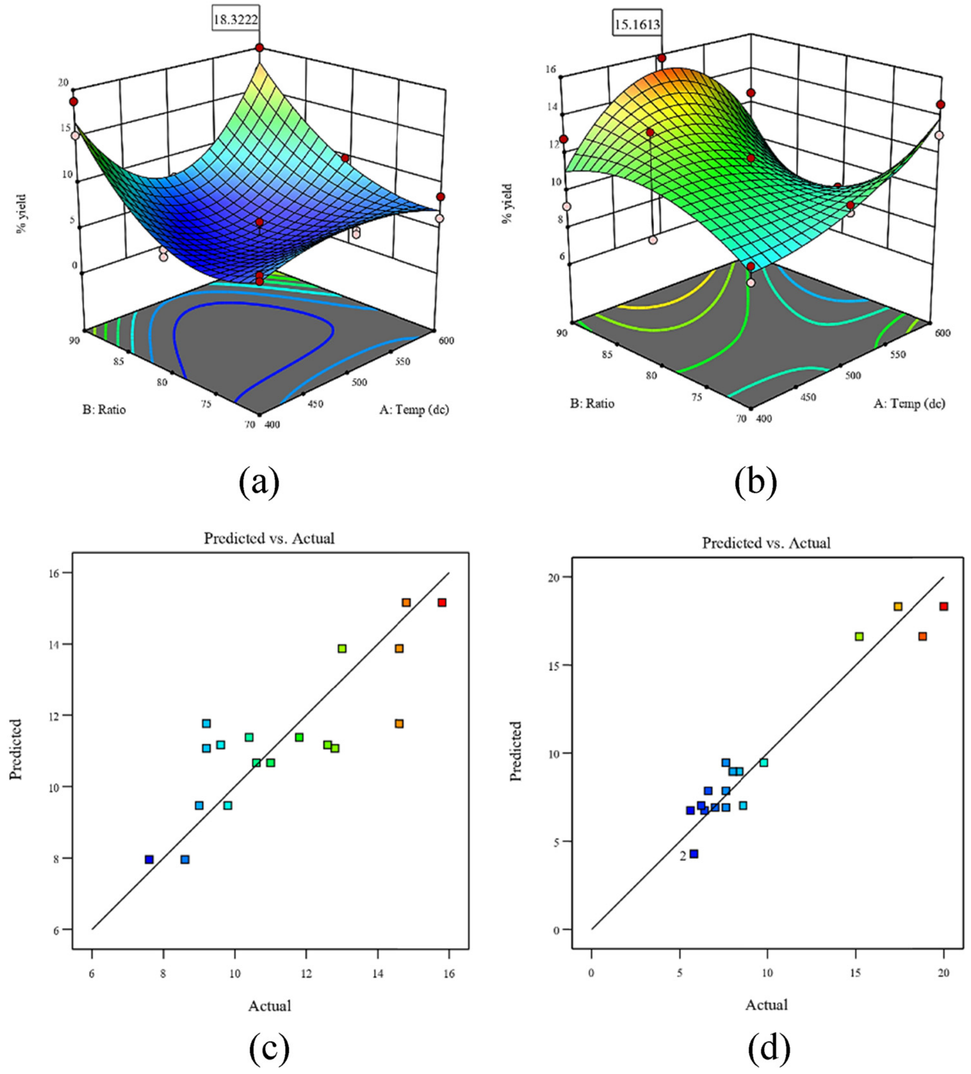

Figure 6: Three-dimensional response surface plots with temperature and mixing-ratio as axes (a) and (b) and the output of the fitted regression model is compared to the actual experimental results for bio-oil yields from CNS (c) and from CFP (d).

Table 4: Main chemical components (according to % peak area) identified by GC-MS in bio-oils from MW pyrolysis of CNS and CFP

Chemical component	CNS	CFP
Acid	0.48	39.13
Esters	0.12	0.15
Ketones	9.18	18.03
Furans	2.65	4.39
Pyrans	0.70	0.39
Guaiacol	7.48	4.17
Syringols	1.14	0.54
Phenol	ND	11.80
(*Z*)-3-(Pentadec-8-en-1-yl)phenol	9.23	ND
2-(5-Methyl-5-hexenyl)phenol	0.75	ND
2-Methoxy-4-vinylphenol	0.57	3.90
3-Tridecylphenol	4.37	ND
4-Chloro-2,3,5-trimethylphenol	0.12	ND
4-Cyclohepta-2,4,6-trienyl-phenol	0.26	ND
Creosol	1.37	4.20
o-Cresol	ND	0.50
Catechol	ND	3.53
p-Cresol	1.25	2.00
Phenol, 2-(1-methylethyl)-	0.64	ND
Phenol, 2,3,5-trimethyl-	1.16	0.00
Phenol, 2,4,6-trimethyl-	0.20	ND
Phenol, 2,4-dimethyl-	3.11	ND
Phenol, 2,6-dimethoxy-	0.91	4.10
Phenol, 2,6-dimethoxy-4-(2-propenyl)-	0.54	0.30
Phenol, 2,6-dimethyl-	0.64	ND
Phenol, 2-ethyl-	4.83	0.20
Phenol, 2-ethyl-4-methyl-	3.18	ND
Phenol, 2-methoxy-	2.33	7.20
Phenol, 2-methoxy-3-methyl-	ND	0.10
Phenol, 2-methoxy-4-(1-propenyl)-	0.73	ND
Phenol, 2-methoxy-4-propyl-	ND	0.30
Phenol, 2-methoxy-6-(2-propenyl)-	ND	0.10
Phenol, 2-methyl-	1.97	ND
Phenol, 3-(1-methylethyl)-	0.54	ND
Phenol, 3-(2-phenylethyl)-	0.30	ND
Phenol, 3,4-dimethoxy-, acetate	ND	0.20
Phenol, 3,4-dimethyl-	0.67	0.30
Phenol, 3,5-dimethyl-, methylcarbamate	ND	0.30
Phenol, 3-cyclohexyl-	2.77	ND
Phenol, 3-dodecyl-	0.61	ND
Phenol, 3-ethyl-	3.76	ND
Phenol, 3-ethyl-5-methyl-	0.84	ND
Phenol, 3-methyl-	6.00	ND
Phenol, 3-octyl-	3.00	ND
Phenol, 3-propyl-	0.79	ND
Phenol, 3-undecyl-	1.18	ND
Phenol, 4-(1-methylethyl)-	0.84	ND
Phenol, 4-ethenyl-2,6-dimethoxy-	ND	0.20
Phenol, 4-ethyl-	1.43	ND
Phenol, diethyl-	1.05	ND
Phenol, *p*-(2-methylallyl)-	0.54	ND
1,2-Benzenediol, 3-methyl-	1.42	0.53
1,2-Benzenediol, 4-methyl-	1.82	0.87

* ND – not detected = concentration below limit of detection.

model-based predictions of bio-oil yields from CNS and CFP are shown in Figure 6a and b, and a flag point indicates the model prediction of run conditions that maximize the yield. It can be seen that the optimal conditions for the production of bio-oil were at 600°C, a ratio of 90:10 (CNS:AC) and a temperature of 500°C; and a ratio of 90:10 (CFP:AC), with the yields estimated as 18.32% and 15.16%, respectively. In Figure 6c and d, the relationships between results from the regression models and the actual experimental results are shown for bio-oil yields from CNS and CFP. The coefficients of determination were $R^2 = 0.9310$ and 0.7125, respectively.

3.6 GC-MS analysis of bio-oil

The chemical composition of bio-oil from MW pyrolysis, analyzed with GC-MS, showed the main components: acids, esters, ketones, furans, pyrans, guaiacol, syringols, and phenols. Most of them are phenol derivatives, as shown in Table 4, listing GC-MS compounds from MW pyrolysis of CNS and CFP optimized to maximal bio-oil yield. Clearly, the bio-oils from CNS and CFP differ in their compositions estimated from peak areas [47]. Significant peak areas in the ion chromatograms were taken by phenolics, acids, ketones, and guaiacol, as shown in Figure 7. For the CNS runs at 400–600°C, it was found that the number of peaks belonging to various chemical constituents was denser than for CFP runs at 400–600°C, and the prominent peak for CFP was attributed to acetic acid.

The analysis of the bio-oils from CNS indicates that the phenolics dominated in the peak area, as shown in Figure 8, contributing 22.37–23.09% for run temperatures from 400°C to 600°C. (*Z*)-3-(pentadec-8-en-1-yl) phenol; phenol, 3-methyl-; phenol, 2-ethyl-; 3-tridecylphenol; and phenol, 3-ethyl- were observed as the main phenolics in bio-oil from CNS. The analysis of bio-oils from CFP indicated that the acids dominated with 37.25–45.20% for temperatures of 400–600°C, as shown in Figure 8. Phenolic compounds were also found, such as phenol; 2-methoxy-4-vinylphenol; phenol, 2,6-dimethoxy-; phenol, 2-methoxy-; etc. The phenolics in pyrolysis bio-oil result from the degradation of complex aromatic scaffolds of lignin [48], and guaiacol or 2-methoxyphenol was an intermediary in the production of *p*-cresol, catechol, and phenol [49]. Guaiacol and syringols are monomeric units of large molecules in lignin, which is broken down during pyrolysis either through demethylation into catechol and methane, or through demethoxylation into phenol and carbon dioxide, according to Wang et al. [50]. Higher phenolics content was found in the CNS bio-oil compared to the CFP bio-oil, because

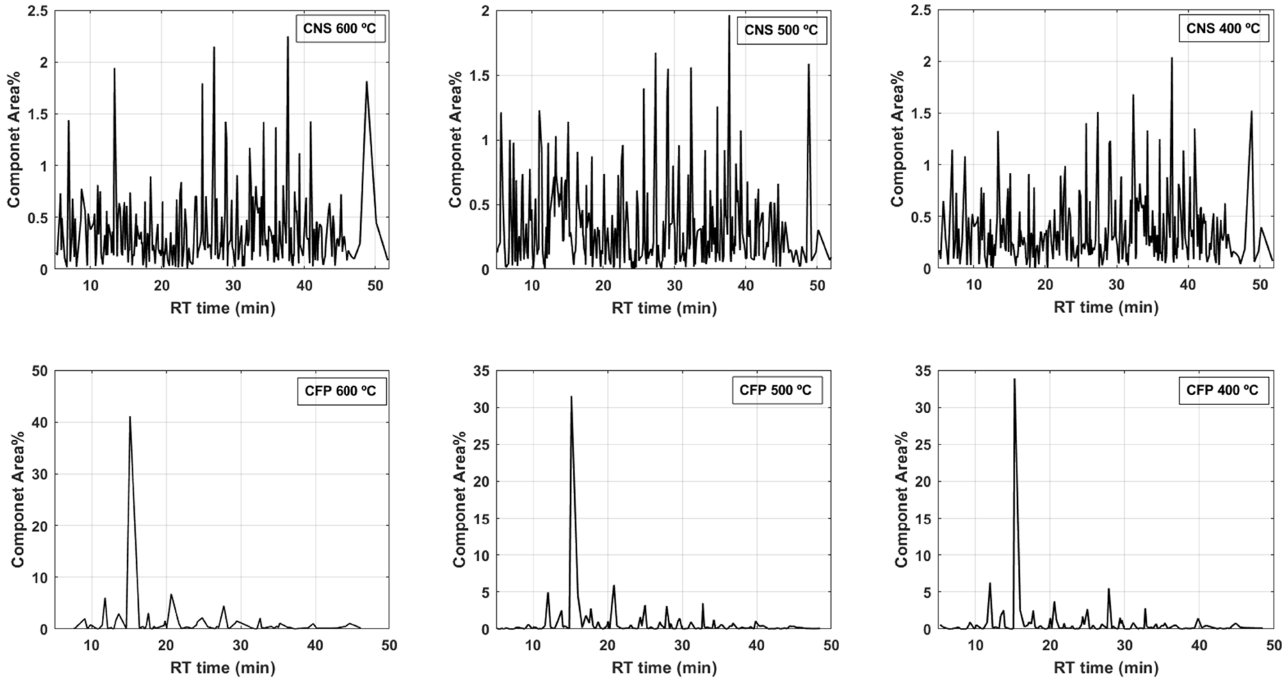

Figure 7: Total ion chromatograms from GC-MS analysis of bio-oils from MW pyrolysis of CNS and CFP.

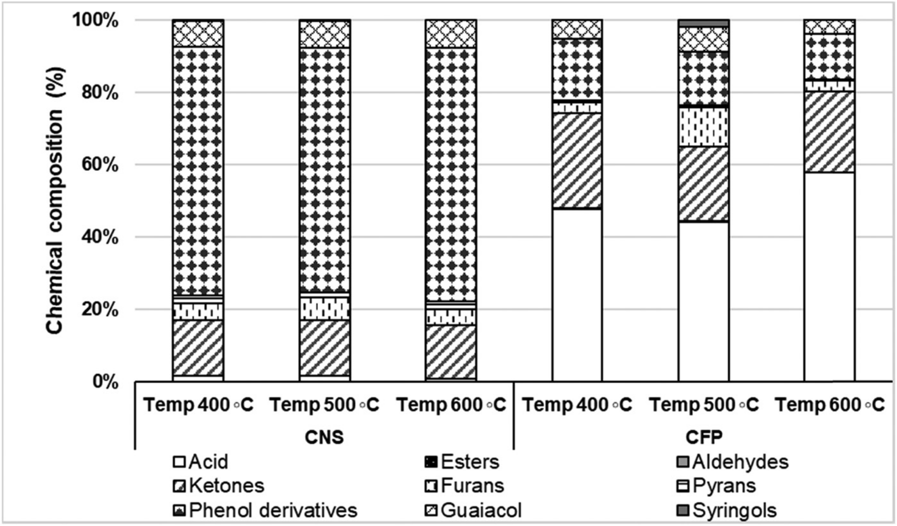

Figure 8: Chemical compositions of bio-oils from the MW pyrolysis of CNS and CFP.

Table 5: Main chemical structural elements in phenol compounds from CNS and CFP bio-oil pyrolysis

Phenol-type (H-type)	Syringol-type (S-type)	Guaiacol-type (G-type)	Catechol-type (C-type)
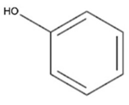	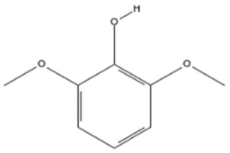	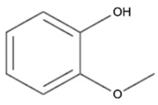	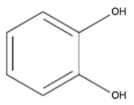
Phenol Phenol, 2-ethyl- Phenol, 4-ethyl- Phenol, diethyl- Phenol, 2,4-dimethyl-	Syringols Phenol, 2,6-dimethoxy- Phenol, 2,6-dimethoxy-4-(2-propenyl)-	Guaiacol Creosol Phenol, 2-methoxy- Phenol, 2-methoxy-3-methyl- 2-Methoxy-4-vinylphenol	Catechol 1,2-Benzenediol, 3-methyl- 1,2-Benzenediol, 4-methyl-

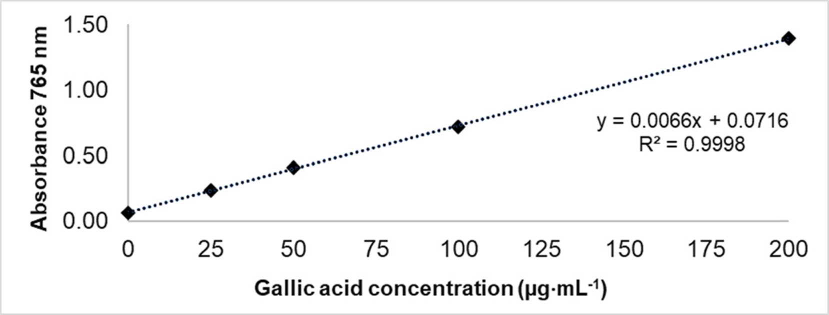

Figure 9: Calibration curve for gallic acid standard in the determination of TPC.

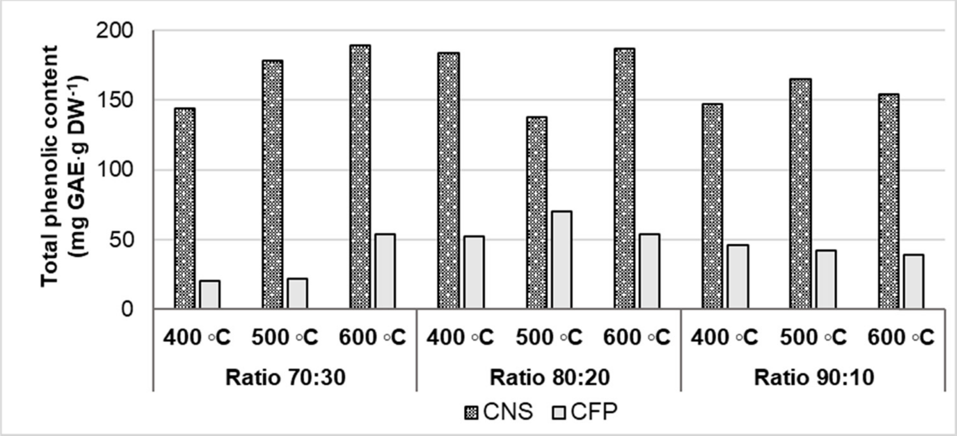

Figure 10: The average TPC of bio-oils from MW pyrolysis of CNS and CFP.

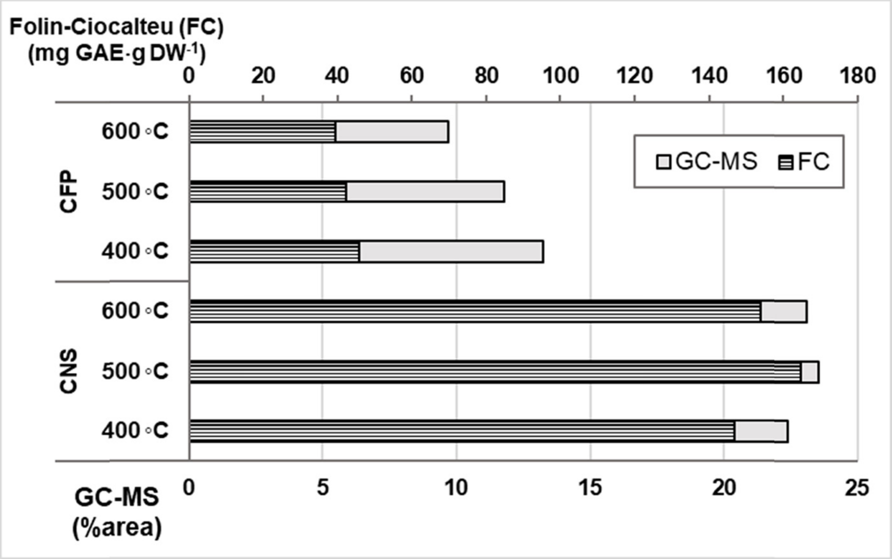

Figure 11: Phenolic contents in bio-oils from MW pyrolysis of CNS and CFP, based on GC–MS and FC analysis.

the CNSL contains polyphenols in CNS and contributes about 30–35% of all CNS [11].

According to the GC-MS chromatography of bio-oils from CNS and CFP, three phenol compounds were obtained, namely phenol, syringol, and guaiacol [51]. Lignin's main chemical components are classified as phenol-type (H-type), syringol-type (S-type), guaiacol-type (G-type), and catechol-type (C-type) compounds [52,53] as presented in Table 5. The catechol-type (C-type) compounds stem from demethylation of guaiacol-type (G-type) [54].

3.7 TPC of bio-oils from FC analysis

The TPC of bio-oils from the MW pyrolysis of CNS and CFP were calculated using the calibration curve for gallic acid, as shown in Figure 9. The gallic acid standards were run at concentrations of 0, 25, 50, 100, and 200 $\mu g \cdot mL^{-1}$, and absorbance was measured at 765 nm wavelength (equation $y = 0.0066x + 0.0716$, $R^2 = 0.9998$) to be 0.067, 0.240, 0.410, 0.720, and 1.392, respectively. The linear fit with a correlation coefficient $r > 0.995$ indicates good linearity of the data [55].

The TPC in bio-oils from MW pyrolysis of CNS and CFP are shown in Figure 10, for run temperatures of 400°C to 600°C. The TPC ranges of these bio-oils from CNS and CFP were 137.67–188.83 mg $GAE \cdot g\ DW^{-1}$ and 20.40–69.90 $mg \cdot GAE \cdot g \cdot DW^{-1}$, respectively. Panitan and Pattawat [56] found in the TPC analysis of five crude extracts (from flowers, young leaves, mature leaves, twigs, and bark of *C. magna*) that the gallic acid calibration curve was suitable ($R^2 = 0.996$), and the TPC in the crude extracts ranged from 0.81 ± 0.09 to 5.73 ± 0.28 $mg \cdot GAE \cdot g \cdot DW^{-1}$. The phenolic content obtained by FC analysis varied depending on the time of basification, compared to gallic acid calibration [57]. The response to FC reagent indicates the number of phenolic groups contained in bio-oil [58].

3.8 Phenolic contents of bio-oils by a different analysis

The bio-oils from CNS and CFP were analyzed by GC-MS and FC analysis. The highest phenolic content in bio-oil from CNS at 500°C was 23.56% and 164.83 mg $GAE \cdot g \cdot DW^{-1}$. Meanwhile, in bio-oil from CFP at 400°C, these were 13.23% and 45.90 mg $GAE \cdot g \cdot DW^{-1}$, as shown in Figure 11. It can be seen that the FC analysis gave a higher phenolic content, partly due to the inaccessible hydroxyl groups. Many researchers have confirmed that this is mainly due to the different responses of different compounds [59].

4 Conclusions

The pyrolysis with MW heating for the production of bio-oil from CNS and CFP was tested experimentally. Within the pyrolysis reactor system, there is an electric field strength of 185.38 $V \cdot m^2$ at an MW frequency of 2.45 GHz, calculated from physical and mathematical model equations using COMSOL MultiphysicsTM program for the simulation that solved the electric field distribution of MW inside the pyrolysis reactor. To study the optimal conditions for the production of bio-oil from the two biomasses, CNS and CFP, while using AC as an MW adsorbent, the experimental design had two manipulated factors, namely temperature (400°C, 500°C, and 600°C) and biomass to AC ratio (70:30, 80:20, and 90:10). It was found that the liquid yields (of total bio-oil) from CNS and CFP increased, respectively, from 6.0% to 18.7% and from 8.1% to 15.3%, over the temperature range from 400°C to 600°C. Experimentally it was found that the ratio of biomass (CNS, CFP) to AC influences the MW pyrolysis, as the ratios 70:30, 80:20, and 90:10 covered yields from low to high. The chemical compositions of bio-oils from CNS and CFP were studied by GC-MS analysis, showing acids, esters, ketones, furans, pyrans, guaiacol, syringol, and phenols as the main components. The bio-oils from CNS and CFP contained phenol derivatives for 23.56% and 13.23%, respectively, derived from the lignin components of phenol-type (H-type), syringol-type (S-type), guaiacol-type (G-type), and catechol-type (C-type). According to FC analysis, the phenolic contents in CNS and CFP bio-oils were maximally 189 and 70 $mg \cdot GAE \cdot g \cdot DW^{-1}$, respectively. According to GC-MS and FC analysis, the CNS bio-oil prepared at 500°C and the CFP bio-oil prepared at 400°C had the highest phenolic contents among the pyrolysis conditions tested.

Funding information: This work was funded by Fundamental Fund 2023 (FF2566; SIT6601171S), and it was supported by Thesis Research Grant for scientific research/development of tools/development of innovations that require materials, Engineering Graduate Scholarship and the authors thank the Research and Development Office (RDO), Prince of Songkla University, Hat-Yai campus, and Prince of Songkla University, Surat-Thani campus for supporting this project under the Integrated High Value of Oleochemical (IH-VO) Research Center.

Author contributions: Ratima Waithongkham processed the experiment, analyzed the results, and drafted a manuscript; Yutthapong Pianroj designed the research methodology; Saysunee Jumrat proposed the method, analyzed results, and drafted a manuscript; Parinuch Chumkaew conducted experiments; Seppo Karrila reviewed the manuscript; Teerasak Punvichai supported the funding research. All the authors read and supervised the final manuscript.

Conflict of interest: The authors state no conflict of interest.

Data availability statement: The authors declare that data supporting the results of this study are contained in additional articles and information.

References

[1] Cherubini F. The biorefinery concept: Using biomass instead of oil for producing energy and chemicals. Energy Convers Manag. 2010;51:1412–21.

[2] Matuchak A, Phongam C. An analysis of renewable energy potential of rural communities in Thailand case study. Academic Artic Eng Technol J Rangsit Univ. 2008;2:25–32.

[3] Kim JS. Production, separation and applications of phenolic-rich bio-oil – A review. Bioresour Technol. 2015;178:90–8.

[4] Stewart D. Lignin as a base material for materials applications: Chemistry, application and economics. Ind Crop Products. 2008;27:202–7.

[5] Huang X, Ludenhoff JM, Dirks M, Ouyang X, Boot MD, Hensen EJM. Selective production of biobased phenol from lignocellulose-derived alkylmethoxyphenols. ACS Catal. 2018;8:11184–90.

[6] Moeiklang N, Ruangviriyachai C. Determination of phenolic compounds and antioxidant potential in fruit beverages. KKU Res J (GS). 2014;14(4):69–79.

[7] Stefanidis SD, Kalogiannis KG, Iliopoulou EF, Michailof CM, Pilavachi PA, Lappas AA. A study of lignocellulosic biomass pyrolysis via the pyrolysis of cellulose, hemicellulose and lignin. J Anal Appl Pyrolysis. 2014;105:143–50.

[8] Yogalakshmi KN, Poornima Devi T, Sivashanmugam P, Kavitha S, Yukesh Kannah R, Sunita Varjani, et al. Lignocellulosic biomass-based pyrolysis: A comprehensive review. Chemosphere. 2022;286:131824.

[9] Karthäuser J, Biziks V, Mai C, Militz H. Lignin and lignin-derived compounds for wood applications—A review. Molecules. 2021;26:2533.

[10] Pongthornpruek S. The utilization of cashew shell residues and grease waste for charcoal briquette production. Appl Environ Res. 2017;39:33–40.

[11] Nyirenda J, Zombe K, Kalaba G, Siabbamba C, Mukela I. Exhaustive valorization of cashew nut shell waste as a potential bioresource material. Sci Rep. 2021;11:11986.

[12] Kyei S, Akaranta O, Darko G, Chukwu U. Extraction, characterization and application of cashew nut shell liquid from cashew nut shells. Chem Sci. 2019;28:1–10.

[13] Das P, Ganesh A. Bio-oil from pyrolysis of cashew nut shell—a near fuel. Biomass Bioenergy. 2003;25:113–7.

[14] Dhamaney C. Development of bamboo boards based on cashew nut shell liquid. Indian Pulp and Paper. 1976;26:20.

[15] Kudwa KG, Kamath NR. Indian Patent. 1948;31:509.

[16] Budaraga IK, Arnim A, Marlida Y, Bulanin U. Analysis of liquid smoke chemical components with GC MS from different raw materials variation production and pyrolysis temperature level. Int J ChemTech Res. 2016;9:694–708.

[17] Neelam C, Ranjan B, Komal S. Antimicrobial activity of *Cassia fistula* Linn. LEGUMES. 2011;2:426–30.

[18] Luximon-Ramma A, Bahorun T, Soobrattee MA, Aruoma OI. Antioxidant activities of phenolic, proanthocyanidin, and flavonoid components in extracts of *Cassia fistula*. J Agric Food Chem. 2002;50:5042–7.

[19] Garg R, Anand N, Kumar D. Pyrolysis of babool seeds (*Acacia nilotica*) in a fixed bed reactor and bio-oil characterization. Renew Energy. 2016;96:167–71.

[20] Akhtar J, Kuang SK, Amin NS. Liquefaction of empty palm fruit bunch (EPFB) in alkaline hot compressed water. Renew Energy. 2010;35:1220–7.

[21] Yaman S. Pyrolysis of biomass to produce fuels and chemical feedstocks. Energy Convers Manag. 2004;45:651–71.

[22] Dhanavath KN, Shah K, Bankupalli S, Bhargava SK, Parthasarathy R. Derivation of optimum operating conditions for the slow pyrolysis of Mahua press seed cake in a fixed bed batch reactor for bio–oil production. J Environ Chem Eng. 2017;5:4051–63.

[23] Kim J-S, Choi G-G. Chapter 11 - Pyrolysis of lignocellulosic biomass for biochemical production. In: Bhaskar T, Pandey A, Mohan SV, Lee D-J, Khanal SK, editors. Waste Biorefinery. Netherlands: Elsevier; 2018. p. 323–48.

[24] Yang H, Yan R, Chen H, Lee DH, Zheng C. Characteristics of hemicellulose, cellulose and lignin pyrolysis. Fuel. 2007;86:1781–8.

[25] Li L, Rowbotham JS, Christopher Greenwell H, Dyer PW. Chapter 8 - An introduction to pyrolysis and catalytic pyrolysis: Versatile techniques for biomass conversion. In: Suib SL. editors. New and Future Developments in Catalysis. Amsterdam: Elsevier; 2013. p. 173–208.

[26] Yin C. Microwave-assisted pyrolysis of biomass for liquid biofuels production. Bioresour Technol. 2012;120:273–84.

[27] Motasemi F, Afzal MT. A review on the microwave-assisted pyrolysis technique. Renew Sustain Energy Rev. 2013;28:317–30.

[28] Prasad K, Jha S, Prakash A. Quality, productivity and business performance in home based brassware manufacturing units. Int J Product Perform Manag. 2015;64:270–87.

[29] Kurian V, Gill M, Dhakal B, Kumar A. Chapter 21 - Recent trends in the pyrolysis and gasification of lignocellulosic biomass. In: Gurunathan B, Sahadevan R. editors. Biofuels and Bioenergy. India: Elsevier; 2022. p. 511–52.

[30] Domínguez A, Menéndez JA, Inguanzo M, Pís JJ. Production of biofuels by high temperature pyrolysis of sewage sludge using conventional and microwave heating. Bioresour Technol. 2006;97:1185–93.

[31] Churin E, Delmon B. What can we do with pyrolysis oils? In Pyrolysis and gasification. London: Elsevier Applied Science; 1989. p. 326–33.

[32] Putun E. Biomass to bio-oil via fast pyrolysis of cotton straw and stalk. Energy Sour. 2002;24(275):285.

[33] Fadhil A. Production and characterization of liquid biofuels from locally available nonedible feedstocks. Asia-Pac J Chem Eng. 2020;16:2572–91.

[34] Alsbou E, Helleur B. Accelerated aging of bio-oil from fast pyrolysis of hardwood. Energy Fuels. 2014;28:3224–35.

[35] Appleton TJ, Colder RI, Kingman SW, Lowndes IS, Read AG. Microwave technology for energy-efficient processing of waste. Appl Energy. 2005;81:85–113.

[36] Folin O, Ciocalteu V. On tyrosine and tryptophane determinations in proteins. J Biol Chem. 1927;73:627–50.

[37] Mishra RK, Mohanty K. Characterization of non-edible lignocellulosic biomass in terms of their candidacy towards

alternative renewable fuels. Biomass Convers Biorefinery. 2018;8:799–812.

[38] Singh YD, Mahanta P, Bora U. Comprehensive characterization of lignocellulosic biomass through proximate, ultimate and compositional analysis for bioenergy production. Renew Energy. 2017;103:490–500.

[39] Abdullah A, Ahmed A, Akhter P, Razzaq A, Zafar M, Hussain M, et al. Bioenergy potential and thermochemical characterization of lignocellulosic biomass residues available in Pakistan. Korean J Chem Eng. 2020;37:1899–906.

[40] Ábrego J, Plaza D, Luño F, Atienza-Martínez M, Gea G. Pyrolysis of cashew nutshells: Characterization of products and energy balance. Energy. 2018;158:72–80.

[41] Tsamba AJ, Yang W, Blasiak W. Pyrolysis characteristics and global kinetics of coconut and cashew nut shells. Fuel Process Technol. 2006;87:523–30.

[42] Lievens C, Mourant D, He M, Gunawan R, Li X, Li C-Z. An FT-IR spectroscopic study of carbonyl functionalities in bio-oils. Fuel. 2011;90:3417–23.

[43] Guedes RE, Luna AS, Torres AR. Operating parameters for bio-oil production in biomass pyrolysis: A review. J Anal Appl Pyrolysis. 2018;129:134–49.

[44] Sharma R, Sheth P. Thermo-chemical conversion of jatropha deoiled cake: Pyrolysis vs. Gasification. Int J Chem Eng Appl. 2015;6:376–80.

[45] Isahak WNRW, Hisham MWM, Yarmo MA, Yun Hin T-Y. A review on bio-oil production from biomass by using pyrolysis method. Renew Sustain Energy Rev. 2012;16:5910–23.

[46] Duan D, Lei H, Wang Y, Ruan R, Liu Y, Ding Y, et al. Renewable phenol production from lignin with acid pretreatment and ex-situ catalytic pyrolysis. J Clean Prod. 2019;231:331–40.

[47] Patra S, Kumar M, Panda A. Production and characterization of Bio oil from Gold Mohar (*Delonix Regia*) seed through pyrolysis process. Int J Ambient Energy. 2016;38:1–21.

[48] Bakar MS, Ahmed A, Jeffery DM, Hidayat S, Sukri RS, Mahlia TM, et al. Pyrolysis of solid waste residues from Lemon Myrtle essential oils extraction for bio-oil production. Bioresour Technol. 2020;318:123913.

[49] Greenhalf CE, Nowakowski DJ, Harms AB, Titiloye JO, Bridgwater AV. Sequential pyrolysis of willow SRC at low and high heating rates – Implications for selective pyrolysis. Fuel. 2012;93:692–702.

[50] Wang S, Dai G, Yang H, Luo Z. Lignocellulosic biomass pyrolysis mechanism: A state-of-the-art review. Prog Energy Combust Sci. 2017;62:33–86.

[51] Sangthong S, Phetwarotai W, Bakar MSA, Cheirsilp B, Phusunti N. Phenol-rich bio-oil from pyrolysis of palm kernel shell and its isolated lignin. Ind Crop Products. 2022;188:115648.

[52] Jin W, Shen D, Liu Q, Xiao R. Evaluation of the co-pyrolysis of lignin with plastic polymers by TG-FTIR and Py-GC/MS. Polym Degrad Stab. 2016;133:65–74.

[53] Yang J-F, Yang C-H, Liang M-T, Gao Z-J, Wu Y-W, Chuang L-Y. Chemical composition, antioxidant, and antibacterial activity of wood vinegar from litchi chinensis. Molecules. 2016;21:1150.

[54] Shen DK, Gu S, Luo KH, Wang SR, Fang MX. The pyrolytic degradation of wood-derived lignin from pulping process. Bioresour Technol. 2010;101:6136–46.

[55] Mashuni M, Akbar TS, Jahiding M. Development of cypermethrin pesticide detection method using ultra violet-visible spectrophotometry. Asian J Chem. 2017;29:346–8.

[56] Panitan S, Pattawat S. Phytochemical screening, determination of total phenolic and flavonoid contents and antioxidant activities from *Crateva magna* (LOUR.) DC; 2018.

[57] Chen LY, Cheng CW, Liang JY. Effect of esterification condensation on the Folin–Ciocalteu method for the quantitative measurement of total phenols. Food Chem. 2015;170:10–5.

[58] Rover M, Brown R. Quantification of total phenols in bio-oil using the Folin–Ciocalteu method. J Anal Appl Pyrolysis. 2013;104:366–71.

[59] Everette JD, Bryant QM, Green AM, Abbey YA, Wangila GW, Walker RB. Thorough study of reactivity of various compound classes toward the Folin−Ciocalteu reagent. J Agric Food Chem. 2010;58:8139–44.